

Development of a traditional Chinese medicine-based agent for the treatment of cancer cachexia

Kun-Chang Wu^{1,2} , Po-Chen Chu³ , Yu-Jung Cheng^{4,5} , Chia-Ing Li^{6,7} , Jingkui Tian^{8,9}, Hsing-Yu Wu¹⁰, Szu-Hsien Wu^{1,11}, Yi-Chun Lai², Hsiang-Han Kao¹² , Ao-Lin Hsu^{2,13,14} , Hsiang-Wen Lin^{1,15,16**†}  & Chih-Hsueh Lin^{6,17**†} 

¹School of Pharmacy, College of Pharmacy, China Medical University, Taichung, Taiwan; ²Research Center for Healthy Aging, China Medical University, Taichung, Taiwan; ³Department of Cosmeceutics and Graduate Institute of Cosmeceutics, China Medical University, Taichung, Taiwan; ⁴Department of Physical Therapy and Graduate Institute of Rehabilitation Science, China Medical University, Taichung, Taiwan; ⁵Department of Rehabilitation, China Medical University Hospital, Taichung, Taiwan; ⁶School of Medicine, College of Medicine, China Medical University, Taichung, Taiwan; ⁷Department of Medical Research, China Medical University Hospital, Taichung, Taiwan; ⁸Institute of Cancer and Basic Medicine, Chinese Academy of Sciences, Cancer Hospital of the University of Chinese Academy of Sciences, Zhejiang Cancer Hospital, Hangzhou, China; ⁹College of Biomedical Engineering & Instrument Science, Zhejiang University, Hangzhou, China; ¹⁰Institute of Biological Chemistry, Academia Sinica, Taipei, Taiwan; ¹¹Institute of New Drug Development, China Medical University, Taichung, Taiwan; ¹²Department of Family Medicine, China Medical University Hospital, Taichung, Taiwan; ¹³PhD Program for Aging, China Medical University, Taichung, Taiwan; ¹⁴Department of Internal Medicine, Division of Geriatrics & Palliative Medicine, University of Michigan Medical School, Ann Arbor, MI, USA; ¹⁵Department of Pharmacy, China Medical University Hospital, Taichung, Taiwan; ¹⁶Department of Pharmacy System, Outcomes and Policy, College of Pharmacy, University of Illinois at Chicago, Chicago, IL, USA; and ¹⁷Department of Geriatric Medicine, China Medical University Hospital, Taichung, Taiwan

Abstract

Background Despite recent advances in understanding the pathophysiology of cancer cachexia, prevention/treatment of this debilitating disease remains an unmet medical need.

Methods We developed an integrated, multi-tiered strategy involving both *in vitro* and *in vivo* muscle atrophy platforms to identify traditional Chinese medicine (TCM)-based anti-cachectic agents. In the initial screening, we used inflammatory cytokine-induced atrophy of C2C12 myotubes as a phenotypic screening platform to assess the protective effects of TCMS. The selected TCMS were then evaluated for their abilities to protect *Caenorhabditis elegans* from age-related reduction of mobility and contractility, followed by the C-26 colon adenocarcinoma mouse model of cachexia to confirm the anti-muscle atrophy effects (body/skeletal muscle weights, fibre size distribution, grip strengths, and serum IL-6). Transcriptome analysis, quantitative real-time polymerase chain reaction, and immunoblotting were performed to gain understanding of the potential mechanism(s) by which effective TCM protected against C26 tumour-induced muscle atrophy.

Results Of 29 widely used TCMS, *Dioscorea radix* (DR) and Mu Dan Pi (MDP) showed a complete protection (all *P* values, 0.0002) vis-à-vis C26 conditioned medium control in the myotube atrophy platform. MDP exhibited a unique ability to ameliorate age-associated decreases in worm mobility, accompanied by improved total body contractions, relative to control (*P* < 0.0001 and <0.01, respectively), which, however, was not noted with DR. This differential *in vivo* protective effect between MDP and DR was also confirmed in the C-26 mouse model. MDP at 1000 mg/kg (MDP-H) was effective in protecting body weight loss (*P* < 0.05) in C-26 tumour-bearing mice without changing food or water intake, accompanied by the restoration of the fibre size distribution of hindleg skeletal muscles (*P* < 0.0001) and the forelimb grip strength (*P* < 0.05). MDP-treated C-26-tumour-bearing mice were alert, showed normal posture and better body conditions, and exhibited lower serum IL-6 levels (*P* = 0.06) relative to vehicle control. This decreased serum IL-6 was associated with the *in vitro* suppressive effect of MDP (25 and 50 µg/mL) on IL-6 secretion into culture medium by C26 cells. RNA-seq analysis, followed by quantitative real-time polymerase chain reaction and/or immunoblotting, shows that MDP's anti-cachectic effect was attributable to its ability to reverse the C-26 tumour-induced re-programming of muscle homeostasis-associated gene expression, including that of two cachexia drivers (MuRF1 and Atrogin-1), in skeletal muscles.

Conclusions All these findings suggest the translational potential of MDP to foster new strategies for the prevention and/or treatment of cachexia. The protective effect of MDP on other types of muscle atrophy such as sarcopenia might warrant investigations.

Keywords Cachexia; Traditional Chinese medicine; Muscle atrophy; C2C12 cell model; C-26 tumour-bearing model; *Caenorhabditis elegans* model

Received: 22 May 2021; Revised: 19 April 2022; Accepted: 13 May 2022

*Correspondence to: Hsiang-Wen Lin, School of Pharmacy, College of Pharmacy, China Medical University, Taichung 406040, Taiwan. Email: hsiangwl@gmail.com; Chih-Hsueh Lin, Department of Geriatric Medicine, China Medical University Hospital, Taichung 406040, Taiwan. Email: d5496@mail.cmuh.org.tw

†Hsiang-Wen Lin and Chih-Hsueh Lin contributed equally to this work as the corresponding authors.

Introduction

A major challenge in the treatment of certain types of cancers, for example, pancreas, stomach, and colon, is the accompanying cancer-induced cachexia, characterized by anorexia and loss of adipose tissues and skeletal muscle masses.¹ Although substantial advances in understanding the multifactorial pathophysiology of cancer cachexia were available, prevention and/or treatment of this debilitating disease remains an unmet medical need. Currently, no approved targeted therapy is available for cachexia, and nutritional support. The semi-synthetic progestational steroid megestrol is the only one agent used to ameliorate cachexia-associated symptoms. A number of Kampo medicines (i.e., multi-component herbal extracts) have been commonly prescribed in Japan to alleviate fatigue and chronic weakness in cachectic patients.² Recently, the hunger hormone ghrelin and ghrelin mimetics have received much attention in light of their potential to enhance appetite and quality of life but lacked clinical evidence to support cachexia treatment.³

The advantage of traditional Chinese medicines (TCMs) over small-molecule targeted agents for the treatment of chronic illnesses is multi-fold. First, the therapeutic utility of the polypharmacology is manifested by their long-standing history in the treatment of various complex diseases.⁴ Second, many TCMs are consumed as dietary supplements on a daily basis. Third, TCMs are generally perceived in oriental societies as having fewer side effects, which might lead to better compliance in patients with chronic diseases.⁵ We performed integrated, multi-tiered strategies to develop TCM-based anti-cachectic agents. We used inflammatory cytokine-induced atrophy of C2C12 myotubes (the C2C12 model)⁶ as a phenotypic screening platform to assess the protective effects of a panel of TCMs. The selected TCMs were then evaluated for their abilities to protect *Caenorhabditis elegans* from age-related reduction of mobility and contractility, based on which the anti-muscle atrophy effect of the candidate TCM was confirmed in the C-26 colon adenocarcinoma mouse model of cachexia (C-26 model).⁷ We found one of the common used TCM, Mu Dan Pi (or Moutan Radicis Cortex; MDP), which exhibited *in vivo* efficacy in protecting C-26 tumour-bearing mice from body weight losses. Mechanistically, RNA-seq and quantitative real-time polymer-

ase chain reaction (qPCR) analysis reveals that MDP's anti-cachectic effect was associated with its ability to reverse the C-26 tumour-induced re-programming of gene expression associated with muscle functions to that of non-cachectic muscles, therefore rescuing skeletal muscles (i.e. two cachexia drivers MuRF1 and Atrogin-1) from wasting. Together, these findings suggest the translational potential of MDP to foster new strategies for the prevention and/or treatment of cachexia in at-risk cancer patients.

Material and methods

Source of the crude extracts of Chinese herbal medicine

Dried root barks of *Paeonia suffruticosa* Andrews (MDP) were purchased from a local herbal medicine store and authenticated by KCW. Crushed MDP was ground into coarse powders (ca. 20 mesh), followed by extraction with 70% methanol (ACS grade; 1 L, three times) at room temperature. The combined supernatants were filtered and concentrated under freeze-drying to generate MDP extracts for further use. We conducted high-performance liquid chromatography fingerprint analysis after each batch of MDP extracts was prepared to ensure batch consistency. All other tested TCM extracts were prepared either by KCW or JKT in a similar manner.

Cell culture

C2C12 myoblasts⁶ and mouse C26 colorectal cancer cells were purchased from the ATCC and maintained in the respective recommended growth media supplemented with 10% fetal bovine serum (Invitrogen, Carlsbad, CA, USA) at 37°C in a humidified incubator containing 5% CO₂.

C26 conditioned medium preparation

Preparation of C26 conditioned medium (C26CM) was conducted according to a reported procedure.^{7,8} Mouse C26

colorectal cancer cells were cultured in 10-cm dishes until reaching 95% confluence, washed twice with PBS, followed by one wash with serum-free DMEM, and grown in serum-free DMEM for 24 h. Collected medium was centrifuging at 1000 *g* for 5 min, filtered through 0.2- μ m syringe filters, and stored at -80°C .

Measurement of myotube width

C2C12 cells were cultured in 6-cm dishes containing 10% PBS in DMEM. When they reached over 95% confluence, the medium was changed to differentiation medium containing 2% horse serum (HS) in DMEM and further cultured for 4 days. The differentiated C2C12 cells were then incubated for additional 4 days in differentiation medium containing C26CM cells (1:1 ratio). The images of differentiated myotubes were obtained by phase-contrast microscopy, and the myotube width was analysed by CellSens Software (Olympus, USA) and represented as percentage of control (%).⁹

Cell viability assays

C26 cells were seeded into 96-well plates at a density of 8×10^3 cells per well in the presence of 10% FBS. After overnight incubation, cells were exposed to MDP at indicated concentrations versus vehicle for 24 h. After treatment, cells were incubated with 3-(4,5-dimethylthiazol-2-yl)-2,5-diphenyltetrazolium bromide (MTT) (Biomatik, Wilmington, DE) for 1 h. The medium was then removed from each well and replaced with DMSO to dissolve reduced MTT dye for subsequent colorimetric measurement of absorbance at 565 nm.

Caenorhabditis elegans mobility test

The age-dependent decline in mobility in *C. elegans* is a well-established model for age-related muscle atrophy,¹⁰ characterized by declines in muscle quantity and quality. The nematode muscle does not contain stem cells, thus providing a suitable model to investigate how the assembled muscle contractile apparatus is maintained during ageing in the absence of regeneration. *Caenorhabditis elegans* undergoes an age-dependent deterioration in the muscle myofilament lattice, which contributes to declines in mobility.¹¹ The microarray analysis has revealed that worm muscle sarcomere proteins undergo an age-dependent decrease starting as early as Day 1 of adulthood.¹² Accordingly, the selected TCM samples were dissolved in either water or 1% DMSO at 10 mg/mL and stored at 4°C (100 \times stock solutions). *Escherichia coli* OP50 bacteria were seeded on fresh NGM plates and left to grow for 2 days. One hundred μL of TCM stock solutions was then added onto NGM plates with OP50 (total volume 10 mL; final TCM concentration, 100 $\mu\text{g}/\text{mL}$). After the TCM

solution was completed absorbed into agar, the OP50 plates were then exposed to UV for 40 min to kill the bacteria. At least 50 synchronized eggs of CF512 worms were seeded on these TCM-containing plates and cultured at 25°C , which was repeated at least three times. Worm videos were recorded on Days 1, 3, 5, and 7 of adulthood. To film the thrashing video of the worms, 2 mL of M9 buffer was added onto the plate. Plates with worms swimming in M9 buffer was then placed under a microscope. The video recording began exactly 2 min after the M9 buffer was added, which last for 1 min. The video was then analysed using ImageJ and wrMTrck (wrMTrck multiple object tracker - phage.dk).¹³

Caenorhabditis elegans body wall muscle contractility assay

To quantify *C. elegans* body wall muscle contraction induced by levamisole, more than 30 worms at different ages (Day 1, 5, 9, and 13 adults) were first incubated in drug-free solution (140 mM NaCl, 5 mM KCl, 5 mM CaCl_2 , 5 mM MgCl_2 , 11 mM dextrose, and 5 mM HEPES; 330 mOsm; pH adjusted to 7.2 with NaOH) and then in levamisole-containing solution (above-mentioned solution with 100 mM levamisole) for 10 min. Images of animals before and after shifting to levamisole-containing solution were taken using regular dissecting scopes with digital imaging system. These images were then used to quantify the length of the worm body using ImageJ. The relative total body contraction was calculated as follows: $[\text{length}_{(\text{before Levamisole})} - \text{length}_{(\text{after levamisole})}] / \text{length}_{(\text{before Levamisole})}$.¹⁴

Experimental animals

Experiments were performed on male CD2F1 mice (approximately 6 weeks of age) obtained from BioLASCO Taiwan Co., Ltd. (Taipei, Taiwan). These mice were kept in the animal centre of China Medical University (CMU) with a controlled temperature of $22 \pm 1^{\circ}\text{C}$ and a relative humidity of $55 \pm 5\%$ under a 12: 12 h light–dark cycle with a rodent diet and clean water *ad libitum*. The experimental protocol was approved by the institutional Animal Care and Use Committee (IACUC) (Protocol No.: CMUIACUC-2018-295).

Colon-26 carcinoma tumour-bearing mouse of cachexia

Previous studies have reported the use of various herbal extracts at 1000 mg/kg,¹⁵ 2000 mg/kg,¹⁶ or so in mice for cancer researches. The dose of 1980 mg/kg was used to study MDP protective effect on cardiac ischaemia/reperfusion in rats.¹⁷ Accordingly, we chose three doses, that is, 100

(MDP-L), 500 (MDP-M), and 1000 mg/kg (MDP-H), for studying the anti-cachectic effect of MDP in C-26 tumour-bearing mice. In addition, H3-14, a small-molecule histone deacetylase (HDAC)3 inhibitor¹⁸ (aka compound 28 in ref. [18]; structure, Figure S1), was used as a positive control based on our previous screening findings. H3-14 was synthesized according to the published procedure,¹⁸ of which the purity ($\geq 98\%$) was verified by nuclear magnetic resonance spectrometry. After an adaptation period of 7 days, CD2F1 mice were randomly divided into the following six groups ($n = 6-10$) for the first set of MDP experiments: (1) normal control group (tumour-free; NC), (2) C26/vehicle group (Veh), (3) C26/H3-14 (100 mg/kg) group, (4) C26/MDP-L group, (5) C26/MDP-M group, and (6) C26/MDP-H group. To investigate the effect of prevention, the treatment groups were respectively pre-treated by oral administration of different doses of MDP or H3-14 (all in 1% carboxymethylcellulose), starting 7 days before C26 cell injection. Mice in the NC and vehicle groups received 1% carboxymethylcellulose only. Tumours were established by the subcutaneous injection of C-26 cells (0.5×10^6 cells in 0.1 mL) into the right flank of mice on Day 7. The tumour volume was measured and calculated using the standard formula ($\text{length} \times \text{width}^2 \times \pi/6$).¹⁹ On the endpoint of this experiment (Day 17), blood and skeletal muscles of quadriceps (Quad), gastrocnemius (GC), and tibialis anterior (TA) samples were collected for analysis.²⁰ In the second set of MDP experiment, tumour-free and C26 tumour-bearing CD2F1 mice were treated with 1% carboxymethylcellulose (NC and Veh) or MDP-H (all $n = 5$) by following the above protocol. Body weights, tumour sizes, and food and water consumptions of individual mice were monitored every other day. At sacrifice, hindleg skeletal muscles were dissected and stored at -80°C for further analysis after body weight measurements. Furthermore, the C26 tumour-bearing experiment of *Dioscoreae* rhizome (DR) was conducted by another batch of CD2F1 mice and divided into the NC ($n = 3$), Vehicle ($n = 6$), and DR ($n = 6$) groups.

IL-6 cytokines in serum

At sacrifice, blood samples were collected via cardiac puncture. After centrifugation at 3500 rpm for 10 min, mouse sera were collected and stored at -80°C until analysis. Serum IL-6 and secreted IL-6 in C26 cell culture medium were measured by using the ELISA MAX[™] Deluxe Set Mouse IL-6 kit (BioLegend, Inc., San Diego, CA, USA).

Grip strength measurement

We measured the grip strength of the forelimbs of mice by using a grip strength meter (Bioseb, Vitrolles, France) as it has been reported that the muscle strength of forelimbs

was comparable to that of hindlimbs in mice in the context of absolute twitch force and maximal isometric tetanic force.²¹ To ensure consistency, the grip strength measurements were carried out by the same person at same day of three different time points. Individual mice were allowed to grip with forelimbs and pulled gently by tails with a consistent force. The maximal strength was recorded when the forelimbs were let go from the grid, and the grip strength was recorded as the average of three measurements.²² However, hindlimbs were used in the following post-mortem analyses due to their larger size relative to forelimbs.

Analysis of fibre cross-sectional area

GC muscles were embedded in paraffin and sectioned at a thickness of 3 μm . Slides were subjected to immunohistochemical staining with anti-dystrophin antibody (ab275391, abcam) to perform qualitative fibre size measurements. Sections were examined and images were captured in a blinded manner with a BX-43 microscope (Olympus America, Melville, NY) outfitted with a SAGE Vision SGHD-3.6C high-resolution digital camera (Sage Vision Co., Ltd, Taipei, Taiwan). ImageJ software (National Institutes of Health, Bethesda, MD) was used to perform quantitative measurements. All of individual muscle fibres were manually traced, and fibre areas of 100–180 muscle fibres were recorded in each slide.

RNA isolation

Total RNA was extracted using a RNeasy kit according to the instruction manual. Purified RNA was quantified at OD260nm using a ND-1000 spectrophotometer (NanoDrop Technology, USA) and qualified by using a Bioanalyzer 2100 (Agilent Technology, USA) with RNA 6000 LabChip kit (Agilent Technology, USA).

Library preparation, sequencing, alignment, and differential expression

Sequencing of mRNAs was performed by a commercial vendor (Welgene Biotech Co., Ltd, Taipei, Taiwan). All RNA sample preparation procedures were carried out according to the Illumina's official protocol (Illumina, USA). Agilent's SureSelect Strand-Specific RNA Library Preparation Kit was used for library construction followed by AMPure XP beads (Beckman Coulter, USA) size selection. The sequence was determined using Illumina's sequencing-by-synthesis technology. Sequencing data (FASTQ reads) were generated using Welgene Biotech's pipeline based on Illumina's basecalling program bcl2fastq v2.20. Both adaptor clipping and sequence quality trimming were performed using Trimmomatic (v0.36).

HISAT2 program was used for mRNA alignment. Differential expression analysis was performed using StringTie (v2.1.3) and Deseq (v1.39.0). Functional enrichment assay in differentially expressed genes of each experiment design was performed using clusterProfiler v3.6. Genes with P value ≤ 0.05 and ≥ 2 -fold changes were considered significantly differentially expressed. The sample reports of RNA QC analysis are attached in *Figure S2*.

qPCR

Total RNA was reverse transcribed to cDNA by using TOOLS Easy Fast RT kit (Biotools, Taipei, Taiwan) according to manufacturer's instructions. qPCR was performed using the CFX Connect Real-time qPCR Detection System (Bio-Rad) with Applied Biosystems™ Power SYBR™ Green PCR Master Mix (Thermo Fisher Scientific). The primer sequences used for quantitative qPCR analysis is attached in *Table S1*.

Immunoblotting

Effect of MDP-H versus vehicle on the protein expression levels of two key muscle cachexia drivers, MuRF1 and Atrogin-1, in skeletal muscles of tumour-bearing mice was examined by immunoblotting. Skeletal muscle tissues were collected and homogenized in lysis buffer containing protease and phosphatase inhibitors. Protein concentrations of muscle lysates were determined by BCA protein assay (Thermo Fisher Scientific, Chicago, IL, USA). Equal amounts of protein samples were separated by SDS-polyacrylamide gel electrophoresis (SDS-PAGE) and electro-transferred onto nitrocellulose membranes. After 1 h blocking with TBST (TBS containing 0.1% Tween 20) containing 5% non-fat milk, membranes were incubated with corresponding primary antibodies at 4°C overnight, washed with TBST buffer three times, and further incubated with secondary antibodies. Signals were visualized with enhanced chemiluminescence substrate (PerkinElmer, Boston, MA, USA).

Statistical analysis

All data were expressed as means with standard deviation or standard error for continuous variables, and frequency or percentages for nominal variables. For experiments with repeated measurements, we applied generalized linear mixed-effects models with random intercept for individual subject and fixed effects for treatment group and days after tumour cell inoculation, accounting for the association of the same measure at different time points from the same subjects. To distinguish differences at each time point among treatment groups, Tukey–Kramer correction for multiple comparisons (e.g. = $0.05/17 = 0.003$ for the multiple compar-

isons with control or vehicle group) was used. For the experiment without repeated measures design, we examined the difference between two groups by using Wilcoxon rank-sum test and the difference among three or more groups by using Kruskal–Wallis test with Dunn's multiple-comparison test using Bonferroni adjustment. For the experiments of *C. elegans* mobility, we applied student's t -test due to a large number of sample sizes. Analysis was conducted by using SAS 9.4 software (SAS, Inc., Cary, NC).

Results

Effects of TCMs on inflammatory cytokine-induced atrophy of C2C12 myotubes

C2C12 murine muscle myoblasts have been proposed as a suitable *in vitro* model for developing therapeutic strategies for the treatment of disease-associated or age-associated muscle wasting.⁶ Thus, we used this C2C12 model as the first-tiered screening platform to assess the protective effect of a panel of 29 TCM extracts on inflammatory cytokine-induced muscle atrophy, in which C26CM served as a source of inflammatory cytokines.⁸ The experimental design is depicted in *Figure 1A*, in which H3-14, a small-molecule HDAC3 inhibitor (aka compound 28),¹⁸ was used as a positive control based on our previous screening findings of a panel of known pan-specific, class I, and isoform-specific HDAC inhibitors obtained from commercial sources or through in-house synthesis. As shown, C26CM caused significant narrowing in C2C12 myotubes, and H3-14 at 1 μ M was effective in counteracting this effect (*Figure 1B* and *1C*).

The selected TCMs (*Table S2*) are traditionally classified as 'heat-clearing, tonifying and replenishing' medicines in light of their diverse health-preserving effects,²³ including hyperglycaemia, anti-oxidation, anti-inflammation, and immunomodulation. Among these TCM extracts, we found two widely used TCMs, DR and MDP, sharing the ability of H3-14 to fully protect C2C12 myotubes from C26CM-induced atrophy (all P s = 0.0002 vis-à-vis C26CM control in the myotube atrophy platform; *Figure 1C*), but other examined TCMs were either cytotoxic or lacked significant protective effects (for full data of those not shown here; *Figure S3*).

Effects of DR and MDP on Caenorhabditis elegans mobility

This phenotypic assay of nematode *C. elegans* demonstrated that MDP, but not DR, could ameliorate age-associated decreases in worm mobility relative to control (*Figure 2A* and *2B*). In a separate experiment, the time-dependent effects of MDP on worm mobility versus total body contractions

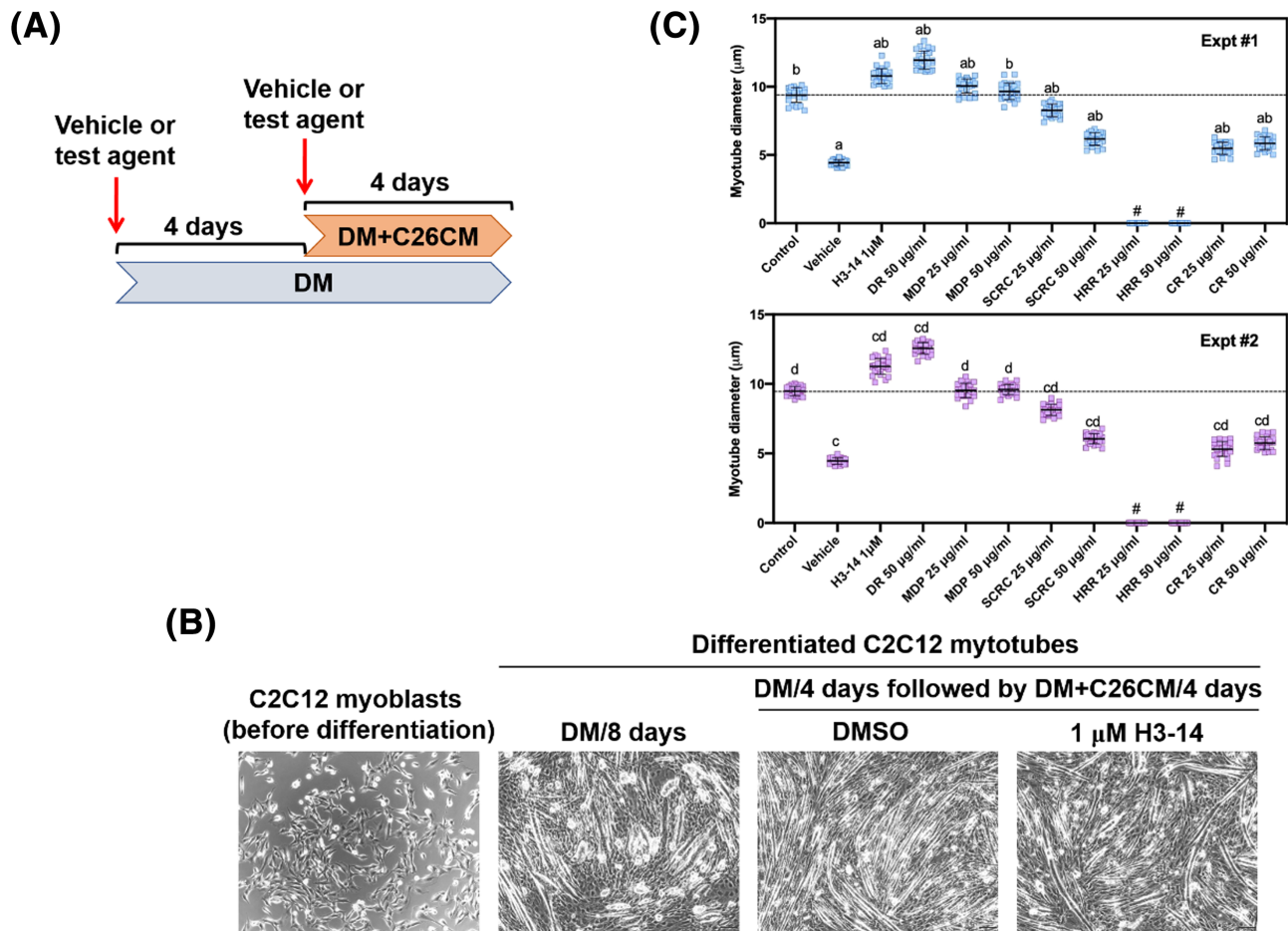


Figure 1 Effects of TCMs on C26CM-induced C2C12 myotube atrophy. (A) Schematic representation of the experimental design. (B and C) Images (B) and quantitative analysis (C) of the protective effect of H3-14 (1 μ M) and/or DR, MDP, and three other representative TCMs on C26CM-induced atrophy of C2C12 myotubes of a representative experiment. Each consisted of multiple measurements of myotube diameters via imaging analysis for individual treatment groups. Bar, means \pm SD (for data obtained from two independent experiments Expt #1 and Expt 2). Note: Significant differences for all pooled data were both compared with the control or vehicle group simultaneously was set at $P < 0.003$ by Wilcoxon rank-sum test with multiple-comparison correction ($\alpha = 0.05/17$ comparisons), instead of at $P < 0.05$. a: $P < 0.003$ as compared with control group; b: $P < 0.003$ as compared with C26CM control (vehicle) in Expt #1; c: $P < 0.003$ as compared with control group; d: $P < 0.003$ as compared with C26CM control (vehicle) in Expt #2. # denotes showed cytotoxic effect. Data of other TCMs examined, which were cytotoxic or lacked protective effects, were shown in Figure S1. CR, *Condonopsis radix*; DM, 2% horse serum-containing differentiation medium; DMSO, dimethyl sulfoxide; DR, *Dioscorea radix*; HRR, *Helminthostachydis radix et rhizome*; MDP, Mu Dan Pi; SD, standard deviation; SCRC, *Sambuci chinensis radix et caulis*; TCM, traditional Chinese medicine.

were analysed to discern whether the ability of MDP to protect the worm mobility was muscle function-related. As shown, MDP showed parallel protective effects in both analyses (Figure 2C and 2D). Together, these findings suggest the unique ability of MDP to delay the rate of age-dependent decline in muscle functions, of which the underlying mechanism might warrant further investigations.

In vivo efficacy of MDP in protecting mice from C26 tumour-induced muscle wasting

In our first set of C-26 model experiments, which was reported to be associated with excessive IL-6 secretion by

the tumour,²⁴ C-26 xenograft tumours were fast growing, approaching the maximally allowable size of 1500 mm³ in our approved IACUC protocol by Day 17 after tumour cell implantation (Figure 3A), due to the aggressive nature of C-26 cancer cells. Therefore, the experiment was terminated at Day 17, at which time all mice were sacrificed. As shown, MDP-H was effective in ameliorating body weight losses in C-26 tumour-bearing mice, which was not noted with the two lower doses (Figure 3A and 3B, with and without tumour mass, respectively; * $P < 0.05$). It is interesting to note that H3-14 did not show any protective effect despite its anti-atrophy effect in the C2C12 myotube model, suggesting complexity in the mechanism that drives muscle wasting *in vivo*. The anti-cachectic activity of MDP-H was not

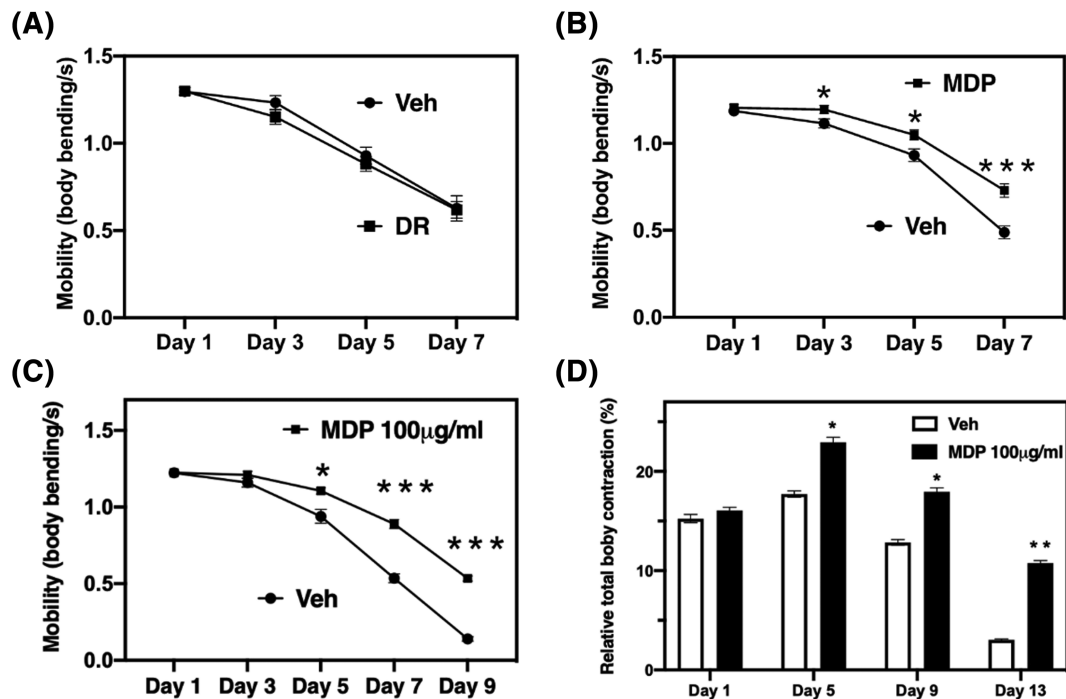


Figure 2 Time-dependent effects of MDP and/or DR on age-associated mobility and/or total body contraction in *Caenorhabditis elegans*. (A) DR versus Veh (B) MDP versus Veh on age-associated decreases in the mobility of *C. elegans* (body bending/second on Days 1, 3, 5, and 7). Data, means \pm SEM. ($n = 170\text{--}420$), $*P < 0.05$; $***P < 0.0001$ (t -test). (C) MDP versus Veh on age-associated decreased in mobility (body bending/second on Days 1, 3, 5, 7, and 9). The error bar denotes SEM. $*P < 0.05$, $***P < 0.0001$ (t -test), $n > 50$. (D) MDP versus Veh on age-associated loss of total body contraction (%). The error bar denotes SEM. $*P < 0.05$, $**P < 0.01$ (t -test), $n > 30$. DR, *Dioscorea radix*; MDP, Mu Dan Pi; SEM, standard error of the mean; Veh, vehicle.

attributable to its ability to reduce tumour burden as MDP-H showed only a very modest tumour-suppressive effect on tumour growth (Figure 3C). Moreover, MDP-H or any other MDP treatment had no significant effect on food or water intake throughout the course of this study (Figure S4), excluding the role of any dietary effect.

Moreover, this protective effect on body weight was paralleled by a similar effect on skeletal muscle weights. As shown in Figure 3D, MDP-H was effective in protecting hind-limb muscles C-26 tumour-bearing mice treated with MDP-M and MDP-H exhibited an alert and active phenotype, lacking signs of cachexia observed in vehicle-treated or H3-14-treated counterparts (hunched posture and rough haircoat) (Figure 3E), despite the finding that MDP-H exhibited no significant suppressive effect on tumour growth. This active phenotype albeit large tumour sizes again underscores the unique anti-cachectic effect of MDP. In contrast, DR at 100 mg/kg exacerbated body weight loss and caused deterioration of physical appearances relative to vehicle control (Figure 4A and 4B), whereas no appreciative effect on tumour growth was noted (Figure 4C).

In the second set of experiments, high-performance liquid chromatography analysis showed an identical pattern of chromatographic fingerprints between two independent preparations of MDP used for the first and second sets of experiments, indicative of consistency in chemical composi-

tions (Figure S5). Consistent with results from the first experiment, MDP-H showed *in vivo* efficacy in protecting mice from C-26 tumour-induced body weight loss with no significant suppressive effect on tumour burden at Day 17 (Figure 5A–C), which was evident by its ability to diminish cachexia-associated decreases in skeletal muscle weights (Figure 5D). Further, MDP-H was able to rescue the fibre size distribution from shifting to smaller cross-sectional areas in cachectic muscles through immunostaining with anti-dystrophin of GC myofibres followed by quantification of myofibre diameter ($P < 0.0001$) (Figure 5E; H&E and anti-dystrophin staining images are shown in Figure S6), accompanied by the restoration of forelimb grip strength at Day 17 in response to MDP-H treatment ($P < 0.001$) (Figure 5F).

MDP exerts the in vivo anti-cachectic effect by reversing tumour-induced re-programming of muscle homeostasis-associated gene expression in skeletal muscles

The mean serum IL-6 (a major driver in the C-26 tumour model of cachexia²⁴) levels in MDP-H-treated C-26 tumour-bearing mice was lower but no statistically significant different from that of vehicle control (Figure 6A, $P = 0.06$).

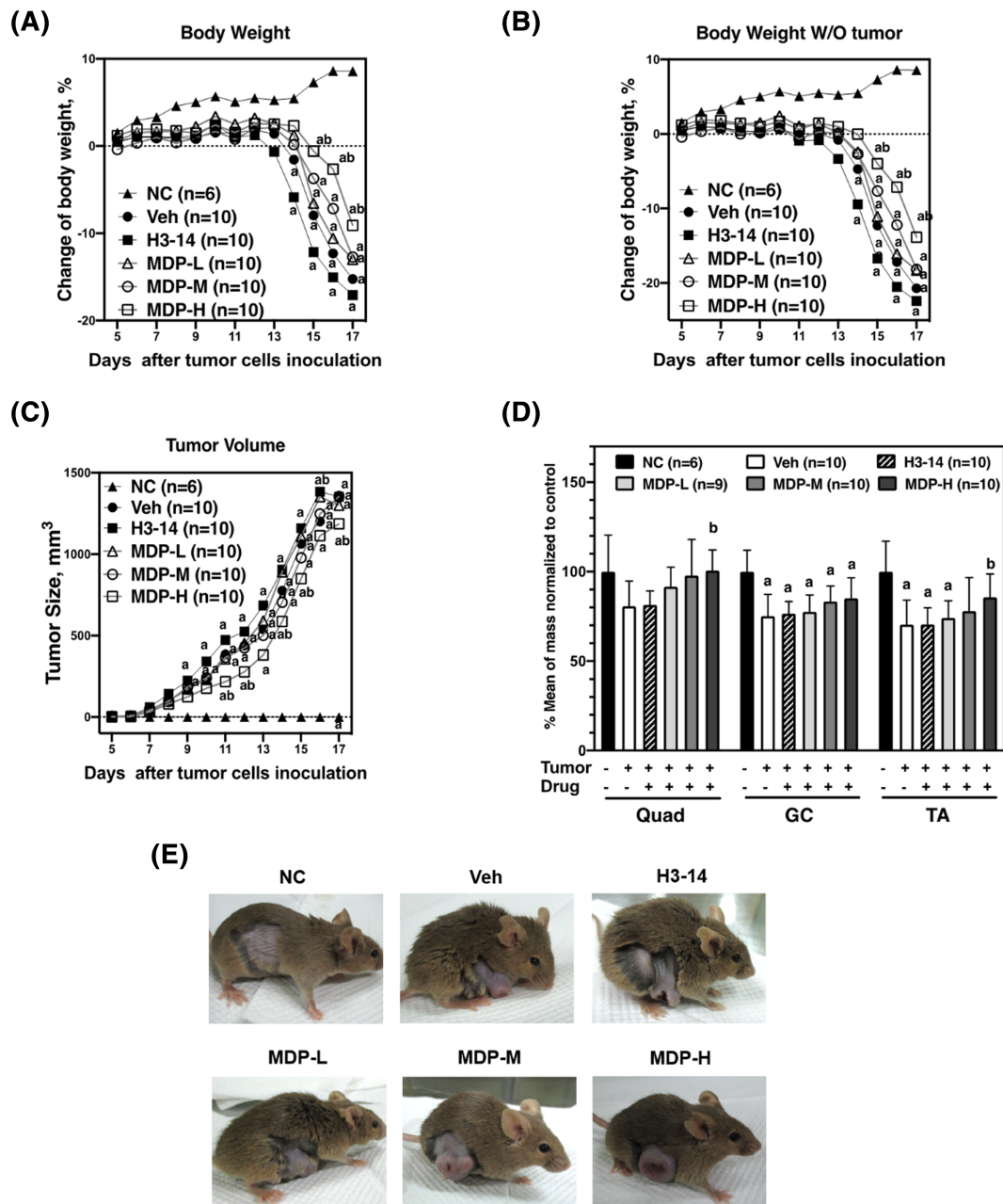


Figure 3 Effects of MDP at three doses (MDP-L, MDP-M, and MDP-H) versus H3-14 and vehicle via oral gavage on the body weight (A and B) and tumour volume (C) of C-26 tumour-bearing mice. Tumour weights were estimated based on the assumption that 1000 mm³ equals to 1 g of body weight. SD bars are not shown to avoid over congestion of these graphs. For statistical analysis, generalized linear mixed-effects models with random intercept for individual subject and fixed effects for treatment and days of the treatment were used to test for differences among groups, using the Tukey–Kramer correction for multiple comparisons. ^aSignificant difference from the control group at $P < 0.05$. ^bSignificant difference from the vehicle group at $P < 0.05$. (D) Effects of MDP at three doses versus H3-14 (100 mg/kg) and vehicle via oral gavage on three different sections of skeletal muscles of hindlegs of C-26 tumour-bearing mice. ^a and ^b denote significant difference from NC group and vehicle group, respectively (Kruskal–Wallis test, with Dunn’s multiple-comparison test using Bonferroni adjustment, $P < 0.05$). © Photographs of one representative mouse from these six groups at the study endpoint depicting the therapeutic effect of MDP-H and MDP-M in tumour-bearing mice, as shown by alertness, normal posture, smooth haircoat, and better body conditions, despite large tumour burdens. DMSO, dimethyl sulfoxide; GC, gastrocnemius muscle; MDP, Mu Dan Pi; MDP-H, MDP high dose as 1000 mg/kg; MDP-L, MDP low dose as 100 mg/kg; MDP-M, MDP median dose as 500 mg/kg; NC, tumour-free mice; Quad, quadriceps femoris muscle; SD, standard deviation; TA, tibialis anterior muscle; Veh, vehicle.

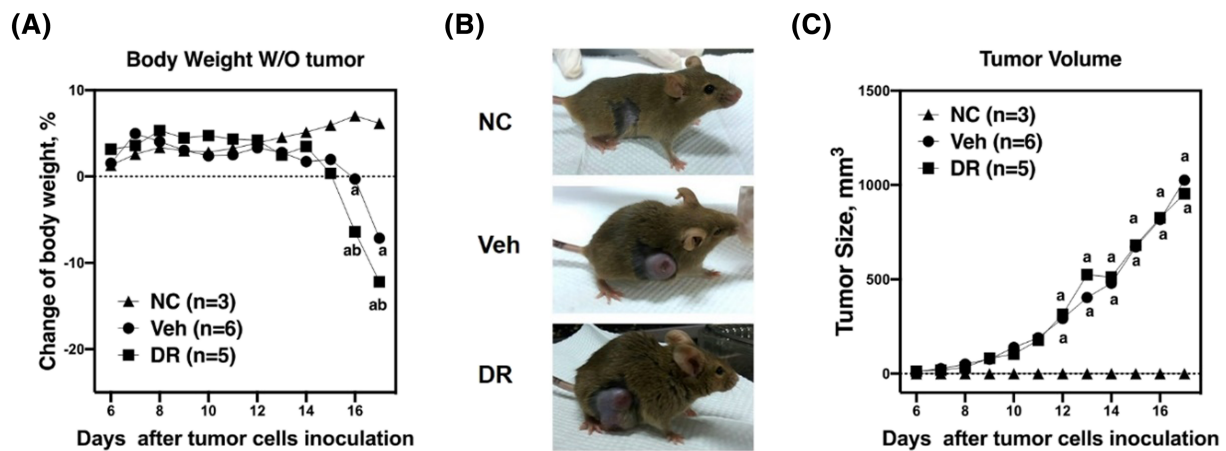


Figure 4 Effects of DR at 100 mg/kg versus vehicle via oral gavage on body weight (w/o tumour) (A) and tumour volume (C) of C-26 tumour-bearing mice ($*P < 0.05$; $n = 3-6$). Control, tumour-free mice. (B) Photographs of representative mice from each group at the study endpoint depicting lack of therapeutic effect of DR. ^a and ^b denote significant difference from the control group and the vehicle group, respectively (generalized linear mixed-effects models with Tukey–Kramer correction for multiple comparisons). DR, *Dioscorea radix*; NC, tumour-free mice; Veh, vehicle.

This diminished serum IL-6 level was associated with the unique ability of MDP at 25 and 50 $\mu\text{g}/\text{mL}$ to suppress IL-6 secretion into culture medium by C26 cells ($P < 0.001$) (Figure 6B). As MDP at these two concentrations was non-cytotoxic to C26 cells (Figure 6C), this MDP-mediated suppression of IL-6 secretion was not attributed to reduced viability of C26 cells (Figure 6C).

The principal component analysis plot shows that the two-dimensional projection of the variation in the T/MDP group was much closer to that of the TF/Veh group than to that of the T/Veh group (Figure 7A). This clustering of expression profiles suggests that MDP was able to shift the gene expression profile of cachectic skeletal muscles (T/Veh) to a state similar to that of non-cachectic muscles (TF/Veh).

Venn diagram analysis reveals a total of 1849 differentially expressed genes shared by the two pairwise comparisons (centre portion) that showed changed expression in the same direction (Figure 7B). Kyoto Encyclopedia of Genes and Genomes pathway enrichment analysis of these 1849 genes revealed that these genes are associated with signalling pathways related to proteasome, autophagy, and protein degradation (Figure 7C, left). Moreover, analysis using the Gene Ontology Knowledgebase shows that these genes are linked to the biological processes of muscle cell differentiation, muscle system process, and muscle tissue development and to the cellular component of proteasomes and lysosomes (Figure 7C, centre and right). These genetic analyses clearly demonstrate the ability of MDP to extensively reprogram the expression of genes associated with muscle homeostasis in cachectic skeletal muscles, which are reflected by the Top 20 most up-regulated versus down-regulated genes in response to MDP treatment (Table S3).

To validate these RNA-seq results, we selected 5 up-regulated and 5 down-regulated genes to conduct qPCR

analysis of skeletal muscles from vehicle-treated versus MDP-H-treated mice, which included the up-regulated genes *Lep*, *Kera*, *Chad*, *Ky*, and *Mettl21e* and the down-regulated genes *Lcn1*, *Mt1*, *Ampd3*, *Fbxo32*, and *Trim63*. Especially noteworthy are *Fbxo32* and *Trim 63*, which encode the two muscle-specific E3 ubiquitin ligases Atrogin-1 and MuRF1, respectively. As shown, changes in the expression levels of these genes from qPCR analysis paralleled that of RNA-seq analysis (Figure 8A). Consistent with the q-PCR results, MDP-H was effective in suppressing the protein expression of Atrogin-1 and MuRF1 in C26 tumour-bearing mice to the basal levels noted in the TF/Veh group upon Western blotting analysis (Figure 8B).

Discussion

At the cellular level, the C2C12 myotube model provided an expedient platform for the initial screening of a panel of TCMs, which allowed us to advance MDP and DR for further assessments in two distinct *in vivo* models. From a drug discovery perspective, *C. elegans* proves to be a useful tool for the phenotypic screening of small-molecule agents/TCMs for ageing,^{12,25} sarcopenia,¹⁰ and a variety of diseases,^{26,27} including cancer,²⁸ infectious diseases,²⁹ and neurodegenerative diseases.^{30,31} Although MDP and DR were both active in the C2C12 myotube model, this *C. elegans* platform was able to discern the differential *in vivo* efficacy of MDP versus DR against muscle atrophy, consistent with results from the C26 mouse model studies.

The extract of DR and its bioactive compound allantoin were reported to regulate the myoblast differentiation and mitochondrial biogenesis of C2C12 myotubes,³² and more

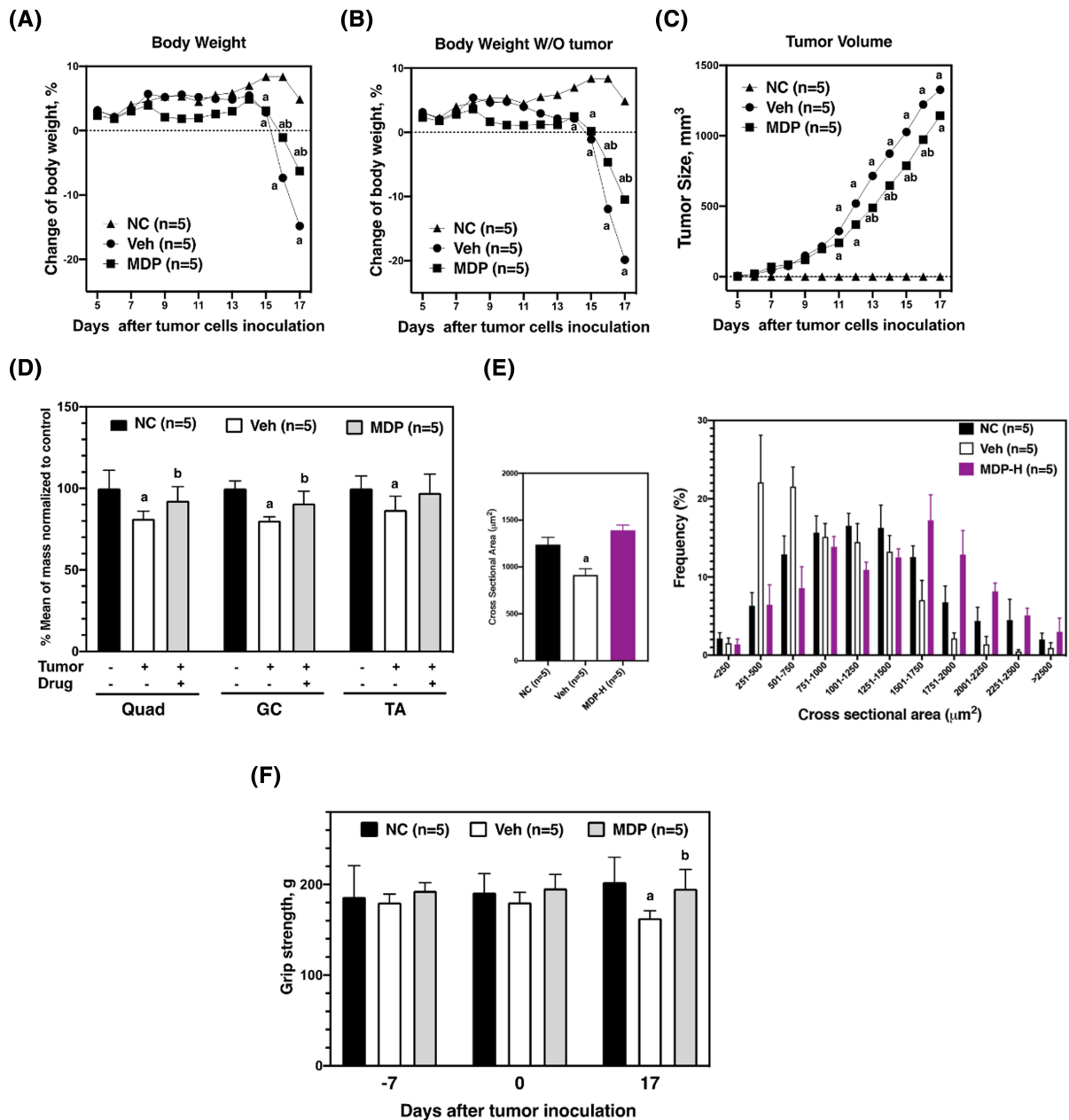


Figure 5 A duplicate experiment showing the effects of MDP at 1000 mg/kg (i.e. MDP-H) versus vehicle via oral gavage on the body weight (A and B) and tumour volume (C) of C-26 tumour-bearing mice. Tumour weights were estimated based on the assumption that 1000 mm³ equals to 1 g of body weight. SD bars are not shown to avoid over-congestion of these graphs. For statistical analysis, generalized linear mixed-effects models with random intercept for individual subject and fixed effects for treatment and days of the treatment were used to test for differences among groups, using the Tukey–Kramer correction for multiple comparisons. ^aSignificant difference from the control group at $P < 0.05$. ^bSignificant difference from the vehicle group at $P < 0.05$. (D) Effects of MDP-H versus vehicle on three different sections of skeletal muscles of hindlegs of C-26 tumour-bearing mice (quad, GC, TA). Control, tumour-free mice. ^a and ^b denote significant difference from control group and vehicle group, respectively (Kruskal–Wallis test, with Dunns multiple-comparison test using Bonferroni adjustment, $P < 0.05$). (E) Effects of MDP-H on the muscle fibre size of GC in C-26 tumour-bearing mice via anti-dystrophin immunostaining followed by quantification of myofibre diameters. Left: Morphometric quantification of the myofibre size. Five sections from the GC muscle of five mice per treatment group were analysed as described in the methods section. ^aThe generalized linear mixed-effects model with random intercept for individual mice and fixed effects for group for testing differences among groups was performed. The comparison between muscles from tumour-bearing/vehicle and tumour-bearing/MDP mice showed statistical significance ($P < 0.0001$). Right: The distribution of cross-sectional areas of muscle fibres in GC muscles represented as a frequency histogram. A multinomial logistic model with correlated responses was fitted to explore the difference level of cross-sectional area among three groups ($P < 0.0001$). (F) Effects of MDP on grip strength measured by the same person on the same day. GC, gastrocnemius muscle; MDP, Mu Dan Pi; MDP-H, MDP high dose as 1000 mg/kg; NC, tumour-free mice; Quad, *quadriceps femoris* muscle; TA, *tibialis anterior* muscle; Veh, vehicle.

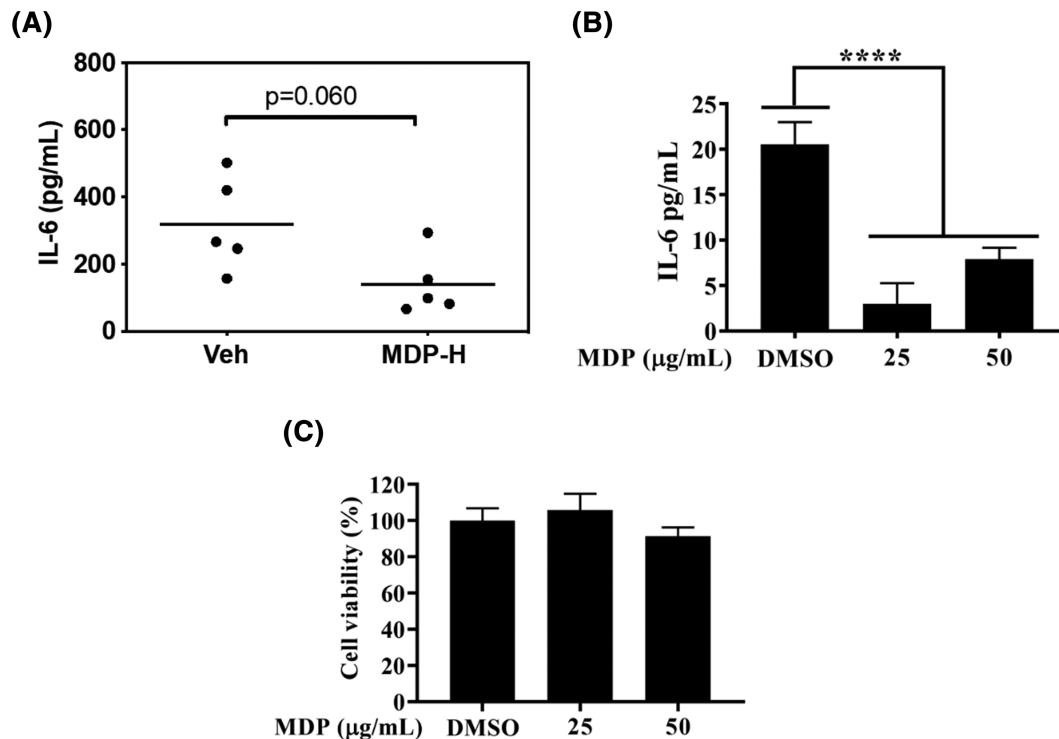


Figure 6 (A) Effects of MDP on serum IL-6 in Veh- versus MDP-H-treated C26-tumour-bearing mice. Wilcoxon rank-sum test was used for statistical analysis ($n = 5$), (B) effects of MDP at 25 and 50 $\mu\text{g/mL}$ on IL-6 production in C26 cell culture medium (C) and on the viability of C26 cells. Bar, mean + SD (for data obtained from three independent experiments for (B) and (C), where **** $P < 0.0001$). DMSO, dimethyl sulfoxide; IL, interleukin; MDP, Mu Dan Pi; MDP-H, MDP high dose as 1000 mg/kg; Veh, vehicle.

recently to improve skeletal muscle dysfunctions in diabetic mice.³³ In this study, although DR was shown to be effective in protecting C2C12 myotubes from C26CM-induced atrophy, this TCM was ineffective in protecting *C. elegans* and C26 tumour-bearing mice from age-related loss of mobility and tumour-induced muscle wasting, respectively. We rationalize that this discrepancy between the *in vitro* and *in vivo* efficacies of DR might be associated with the presence of steroidogenic and oestrogen-stimulating compounds in this TCM.³⁴ Pharmacologically, these compounds might stimulate C2C12 myoblast differentiation and/or myotube proliferation but are ineffective in protecting against loss of muscle functions or muscle wasting in whole animal models.

RAN-seq analysis in conjunction with qPCR and Western blot analyses suggests that MDP's anti-cachectic effect could be attributable to its ability to reverse tumour-induced re-programming of genes governing muscle homeostasis, shifting the expression pattern similar to that of healthy muscles. This extensive genetic re-programming is reminiscent to that reported with the pan-histone deacetylase (HDAC) inhibitor AR-42 in C26 tumour-bearing mice.¹⁷ Nevertheless, the involvement of HDAC inhibition in MDP-mediated anti-cachectic effect was refuted by the inability of MDP to induce histone H3 hyperacetylation in cells (Figure S7). We hypothesize that MDP might act by altering the activation

status/expression of relevant transcription factors to induce such an extensive genetic re-programming.

Bioinformatic analyses of the 1849 differentially expressed genes shared by the two pairwise comparisons (Figure 7B) revealed that most of these genes were linked to pathways/biological processes associated with muscle homeostasis. For example, the products of the top two most up-regulated genes are two chemokines Ccl21 and Ccl12 (Table S3), which act as chemoattractants through the respective receptors Ccr7³⁵ and Ccr2³⁶ in immune cells. Evidence suggests that these two chemokine receptors might be involved in regulating energy expenditure and muscle regeneration, respectively. Conversely, the products of several Top 20 most down-regulated genes in MDP-treated mice have been reported as pathological mediators or key players in cancer-induced cachexia (Table S3). Specifically, the expression levels of MuRF1 and Atrogin-1, the selective muscle cachexia driver genes from skeletal muscle samples, were effectively reverted in MDP-H-treated tumour-bearing mice, as compared with that in vehicle-treated tumour-bearing mice. The ability of MDP to down-regulate the expression of these two cachexia drivers might represent the direct cause for its anti-cachectic effect in light of the finding in a recent study.³⁷ It is worth mentioning that the mode of action of MDP in targeting the expression of muscle

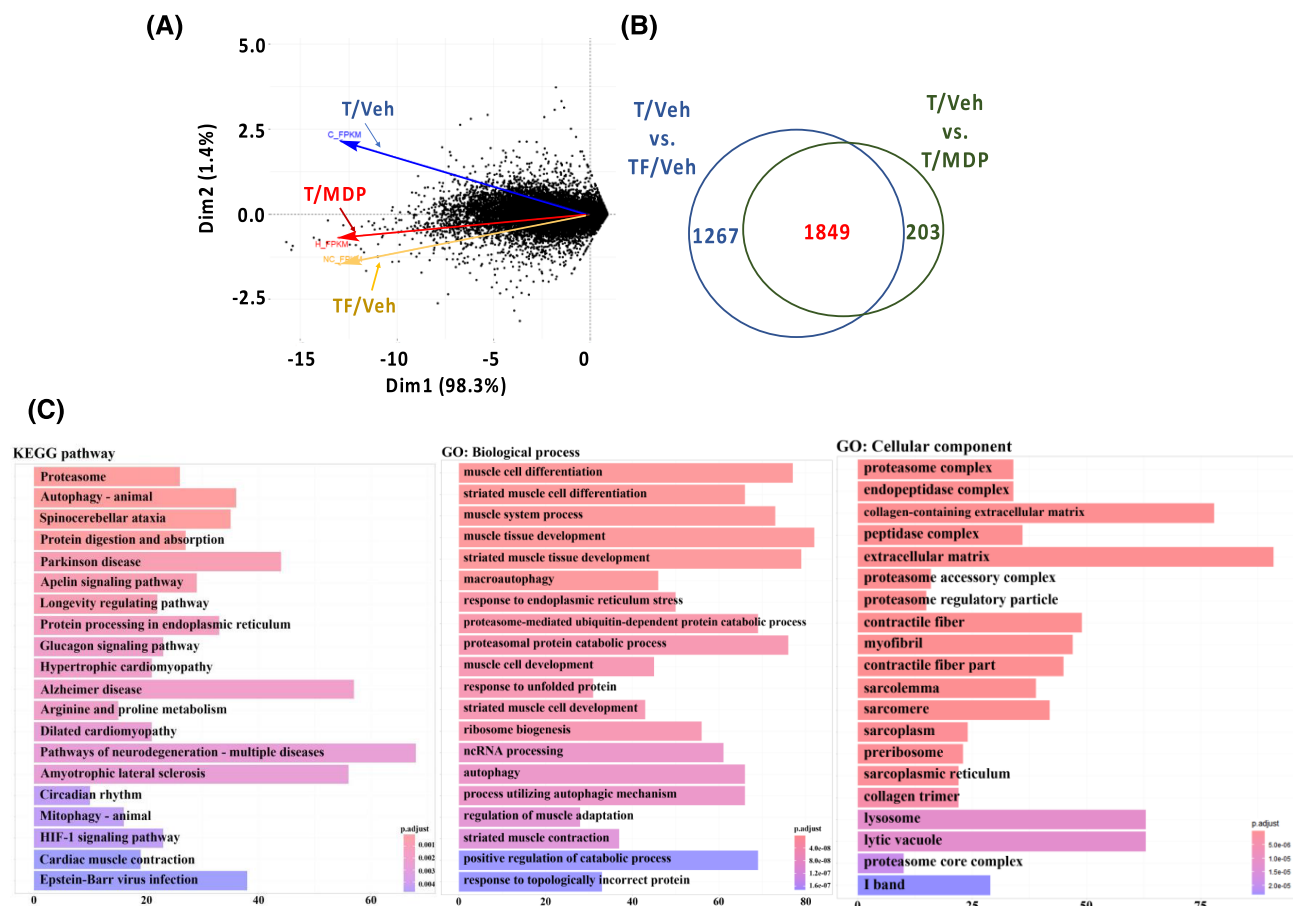


Figure 7 Gene expression in skeletal muscles via RNA sequencing (RNA-seq). (A) Two-dimensional projection of RNA-seq data from the three study groups. The principal component analysis axes (Dim1, x-axis; Dim2, y-axis) emphasize the overall variation in RNA-seq data. Each black dot represents a transformed gene expression value. (B) Venn diagram of differentially expressed genes in each of the two pairwise comparisons of T/Veh versus TF/Veh and T/Veh versus T/MDP. (C) KEGG pathways analysis (left), GO biological process analysis (centre), and GO cellular component analysis (right) of the 1849 differentially expressed genes shared by the above two pairwise comparisons. Dim, dimension; GO, gene ontology; KEGG, Kyoto Encyclopedia of Genes and Genomes; MDP, Mu Dan Pi; RNA-seq, RNA sequencing; T, tumour; TF, tumour-free; Veh, vehicle.

homeostasis-associated genes appears to be different from the adaptogenic effects of Kampo medicines,² which warrants further investigation to explore the possibility of therapeutic combinations. It is worth mentioning that the daily dose of MDP at 1000 mg/kg (MDP-H) in mice is attainable for human consumption. According to the US Food and Drug Administration (FDA) guideline,³⁸ a factor of 0.08 is used when translating a dose used in mice to the human equivalent dose in a clinical trial setting. Consequently, a daily dose of 6.4 g of MDP will be needed for a person with an average weight of 80 kg ($= 1 \text{ g}(1000 \text{ mg})/\text{kg} \times 0.08 \times 80 \text{ kg}$), which is within the daily range of 6–12 g prescribed as a TCM depicted in the Taiwan Herbal Pharmacopoeia.²³

This study is limited by lack of a clear understanding of the mechanism by which MDP regulate the expression of such a diverse array of muscle homeostasis-associated genes. Although the anti-muscle atrophy effect of MDP has been verified in the integrated, multi-tiered strategy, we would like

to test the *in vivo* efficacy of MDP in another mouse model of cachexia (e.g. the newly developed mouse model of pancreatic adenocarcinoma-induced cachexia)³⁹ to help shed light onto MDP's underlying mechanism in the future. In addition, the effect of MDP-H on tumour-specific pro-cachectic factors remains uncharacterized, which might also contribute to the reversal of cachectic phenotype or genotype in C-26 tumour-bearing mice (i.e. protective effect on the driver genes of MuRF1 and Atrogin-1 against cancer cachexia). For example, MDP-H could reduce the level of circulating IL-6, though not statistically significant, in C26 tumour-bearing mice. We obtained evidence that MDP was effective in blocking IL-6 secretion in the culture medium of C26 cells. Together with the findings that MDP-H could protect C2C12 myoblasts from C26CM-induced atrophy, we rationalize that the mechanism by which MDP exerts its anti-cachectic effect might be twofold by acting on tumours and skeletal muscles in a concerted manner, which warrants further investigations.

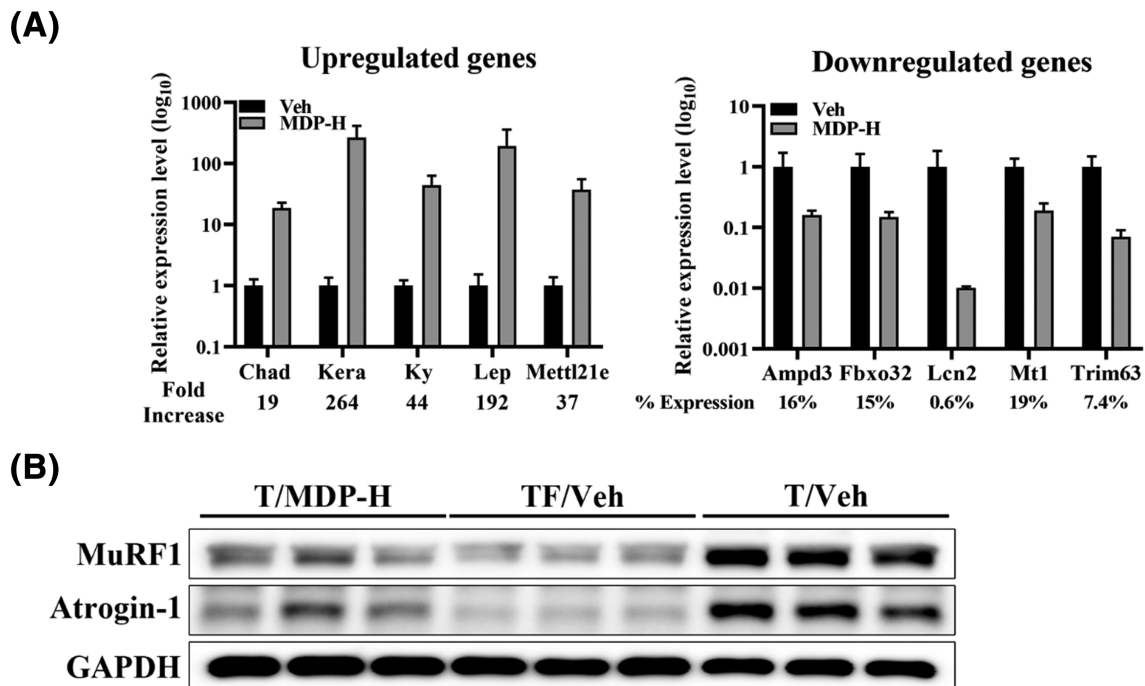


Figure 8 Effects of MDP on skeletal muscle-related genes and protein expressions. (A) qPCR analysis of five up-regulated (left) and five down-regulated (right) genes in skeletal muscles from vehicle-treated versus MDP-H-treated mice ($n = 3$ for each group), where fold increase and % expression on up-regulated and down-regulated genes, respectively, were relative expression levels of selected skeletal muscle-related genes of MDP-H-treated mice to the vehicle counterparts. Bar, means + SD ($n = 3$) (B) Western blot analysis of the protein expression levels of MuRF1 and Atrogin-1 in skeletal muscles from vehicle-treated and MDP-H-treated C26 tumour-bearing mice (T/Veh and T/MDP-H, respectively) vis-à-vis vehicle-treated tumour-free mice (TF/Veh). GAPDH, glyceraldehyde 3-phosphate dehydrogenase; MDP, Mu Dan Pi; MDP-H, MDP high dose as 1000 mg/kg; MuRF1, muscle RING-finger protein-1; qPCR, quantitative real-time polymerase chain reaction; Veh, vehicle.

Another limitation is that it is unclear whether a single constituent or multiple compounds mediate MDP's anti-cachectic effect. Accordingly, further purification of MDP extracts via solvent fractionation in tandem with different types of column chromatography is currently underway. We expect that such information will help foster new strategies of combining MDP with chemotherapeutic regimens for the treatment of cancer patients at risk of cachexia or further to explore the effects of MDP on ageing-related sarcopenia.

Acknowledgements

The authors also would like to extend their gratitude to Yu-Zhen Chou, Pei-Chun Lin, and Professor Yang Liang-Yo for their involvement and contribution in this research. We appreciate the help from CMU Medicinal Chemistry Core facility in synthesizing H3-14.

Funding

This research was partially supported by China Medical University (CMU) (CMU108-Z-7, CMU109-Z-07, CMU110-Z-

07), China Medical University Hospital (DMR-110-080), and Ministry of Science and Technology (MOST 109-2622-8-039-001-TB1 and MOST 110-2622-8-039-004-TB1) and by the "Drug Development Center, China Medical University" from The Featured Areas Research Center Program within the framework of the Higher Education Sprout Project by the Ministry of Education (MOE), in Taiwan. The listed funding agencies had no role in the study implementation, analysis or interpretation of data, or preparation, review or approval of the manuscript. We would like to appreciate all the assistances, researchers and experts in this project.

Conflict of interest

The authors declare no conflict of interest.

Author contributions

KCW, PCC, YJC, HWL, and CHL designed the study. KCW, PCC, YJC, JKT, HYW, SHW, ALH, and YCL performed the experiments. KCW, PCC, CIL, CIL, HHK, HWL, and CHL wrote the manuscript. KCW, PCC, CIL, CIL, HHK, HWL, and CHL

revised the manuscript. All authors read and approved the final manuscript. The authors certify that they comply with the ethical guidelines for authorship and publishing of the *Journal of Cachexia, Sarcopenia and Muscle*.⁴⁰

Online supplementary material

Additional supporting information may be found online in the Supporting Information section at the end of the article.

References

- Baracos VE, Martin L, Korc M, Guttridge DC, Fearon KCH. Cancer-associated cachexia. *Nat Rev Dis Primers* 2018; **4**:17105.
- Kuchta K, Cameron S. Phytotherapy for cachexia: Where do we stand? *Front Pharmacol* 2020; **11**:917.
- Mansson JV, Alves FD, Biolo A, Souza GC. Use of ghrelin in cachexia syndrome: A systematic review of clinical trials. *Nutr Rev* 2016; **74**:659–669.
- Zhang R, Zhu X, Bai H, Ning K. Network pharmacology databases for traditional Chinese medicine: Review and assessment. *Front Pharmacol* 2019; **10**:123.
- Lam TP. Strengths and weaknesses of traditional Chinese medicine and Western medicine in the eyes of some Hong Kong Chinese. *J Epidemiol Community Health* 2001; **55**:762–765.
- Sharples AP, Al-Shanti N, Stewart CE. C2 and C2C12 murine skeletal myoblast models of atrophic and hypertrophic potential: Relevance to disease and ageing? *J Cell Physiol* 2010; **225**:240–250.
- Aulino P, Berardi E, Cardillo VM, Rizzuto E, Perniconi B, Ramina C, Padula F, Spugnini EP, Baldi A, Faiola F, Adamo S, Coletti D. Molecular, cellular and physiological characterization of the cancer cachexia-inducing C26 colon carcinoma in mouse. *BMC Cancer* 2010; **10**:363.
- Seto DN, Kandarian SC, Jackman RW. A key role for leukemia inhibitory factor in C26 cancer cachexia. *J Biol Chem* 2015; **290**:19976–19986.
- Li W, Moylan JS, Chambers MA, Smith J, Reid MB. Interleukin-1 stimulates catabolism in C2C12 myotubes. *Am J Physiol Cell Physiol* 2009; **297**:C706–C714.
- Christian CJ, Benian GM. Animal models of sarcopenia. *Aging Cell* 2020; **19**:e13223.
- Glenn CF, Chow DK, David L, Cooke CA, Gami MS, Iser WB, Hanselman KB, Goldberg IG, Wolkow CA. Behavioral deficits during early stages of aging in *Caenorhabditis elegans* result from locomotory deficits possibly linked to muscle frailty. *J Gerontol A Biol Sci Med Sci* 2004; **59**:1251–1260.
- Mergoud dit Lamarche A, Molin L, Pierson L, Mariol MC, Bessereau JL, Gieseler K, Solari F, Mariol MC, Solari F. UNC-120/SRF independently controls muscle aging and lifespan in *Caenorhabditis elegans*. *Aging Cell* 2018; **17**:e12713.
- Gaffney CJ, Bass JJ, Barratt TF, Szewczyk NJ. Methods to assess subcellular compartments of muscle in *C. elegans*. *J Vis Exp* 2014; **93**:e52043.
- Liu J, Zhang B, Lei H, Feng Z, Liu J, Hsu AL, Xu XZS. Functional aging in the nervous system contributes to age-dependent motor activity decline in *C. elegans*. *Cell Metab* 2013; **18**:392–402.
- Al-Affif N, Alabsi A, Kaid F, Bakri M, Ramanathan A. Prevention of oral carcinogenesis in rats by *Dracaena cinnabari* resin extracts. *Clin Oral Investig* 2019; **23**:2287–2301.
- Fang T, Fang Y, Xu X, He M, Zhao Z, Huang P, Yuan F, Guo M, Yang B, Xia J. *Actinidia chinensis* Planch root extract attenuates proliferation and metastasis of hepatocellular carcinoma by inhibiting epithelial-mesenchymal transition. *J Ethnopharmacol* 2019; **231**:474–485.
- Dan H, Zhang L, Qin X, Peng X, Wong M, Tan X, Yu S, Fang N. Moutan cortex extract exerts protective effects in a rat model of cardiac ischemia/reperfusion. *Can J Physiol Pharmacol* 2016; **94**:245–250.
- Hsieh H-Y, Chuang H-C, Shen F-H, Detroja K, Hsin L-W, Chen C-S. Targeting breast cancer stem cells by novel HDAC3-selective inhibitors. *Eur J Med Chem* 2017; **140**:42–51.
- Gumucio JP, Mendias CL. Atrogin-1, MURF-1, and sarcopenia. *Endocrine* 2013; **43**:12–21.
- Tseng Y-C, Kulp SK, Lai I-L, Hsu E-C, He W-A, Frankhouser DE, Yan PS, Mo X, Bloomston M, Lesinski GB, Marcucci G, Guttridge DC, Bekaii-Saab T, Chen CS. Preclinical investigation of the novel histone deacetylase inhibitor AR-42 in the treatment of cancer-induced cachexia. *J Natl Cancer Inst* 2015; **107**:djv274.
- Takeshita H, Yamamoto K, Nozato S, Inagaki T, Tsuchimochi H, Shirai M, Yamamoto R, Imaizumi Y, Hongyo K, Yokoyama S, Takeda M, Oguro R, Takami Y, Itoh N, Takeya Y, Sugimoto K, Fukada SI, Rakugi H. Modified forelimb grip strength test detects aging-associated physiological decline in skeletal muscle function in male mice. *Sci Rep* 2017; **7**:42323.
- Kim H, Cho SC, Jeong H-J, Jeong H-J, Lee H-Y, Jeong MH, Pyun JH, Ryu D, Kim MS, Lee YS, Kim MS, Park SC, Lee YI, Kang JS. Indoprofen prevents muscle wasting in aged mice through activation of PDK1/AKT pathway. *J Cachexia Sarcopenia Muscle* 2020; **11**:1070–1088.
- Ministry of Health and Welfare. *Taiwan Herbal Pharmacopeia*, 3rd Edition English Version. Taiwan, Taipei: Ministry of Health and Welfare Taiwan, Republic of China; 2019.
- Carson JA, Baltgalvis KA. Interleukin 6 as a key regulator of muscle mass during cachexia. *Exerc Sport Sci Rev* 2010; **38**:168–176.
- Liu H, Guo M, Xue T, Guan J, Luo L, Zhuang Z. Screening lifespan-extending drugs in *Caenorhabditis elegans* via label propagation on drug-protein networks. *BMC Syst Biol* 2016; **10**:131.
- O'Reilly LP, Luke CJ, Perlmutter DH, Silverman GA, Pak SC. *C. elegans* in high-throughput drug discovery. *Adv Drug Deliv Rev* 2014; **69**:247–253.
- Carretero M, Solis GM, Petrascheck M. *C. elegans* as model for drug discovery. *Curr Top Med Chem* 2017; **17**:2067–2076.
- Bae Y-K, Sung J-Y, Kim Y-N, Kim S, Hong K-M, Kim H-T, Choi MS, Kwon JY, Shim J. An in vivo *C. elegans* model system for screening EGFR-inhibiting anti-cancer drugs. *PLoS ONE* 2012; **7**:e42441.
- Kim W, Hendricks GL, Lee K, Mylonakis E. An update on the use of *C. elegans* for preclinical drug discovery: Screening and identifying anti-infective drugs. *Expert Opin Drug Discovery* 2017; **12**:625–633.
- Ikenaka K, Tsukada Y, Giles AC, Arai T, Nakadera Y, Nakano S, Kawai K, Mochizuki H, Katsuno M, Sobue G, Mori I. A behavior-based drug screening system using a *Caenorhabditis elegans* model of motor neuron disease. *Sci Rep* 2019; **9**:10104.
- Chen X, Barclay JW, Burgoyne RD, Morgan A. Using *C. elegans* to discover therapeutic compounds for ageing-associated neurodegenerative diseases. *Chem Cent J* 2015; **9**:65.
- Ma J, Kang SY, Meng X, Kang AN, Partk JH, Park Y-K, Park YK, Jung HW. Effects of rhizome extract of *Dioscorea batatas* and its active compound, allantoin, on the regulation of myoblast differentiation and mitochondrial biogenesis in C2C12 myotubes. *Molecules* 2018; **23**:2023.
- Ma J, Meng X, Liu Y, Yin C, Zhang T, Wang P, Park YK, Jung HW. Effects of a rhizome aqueous extract of *Dioscorea batatas* and its bioactive compound, allantoin in high

- fat diet and streptozotocin-induced diabetic mice and the regulation of liver, pancreas and skeletal muscle dysfunction. *J Ethnopharmacol* 2020;**259**:112926.
34. Lu J, Wong RN, Zhang L, Wong RYL, Ng TB, Lee KF, Zhang YB, Lao LX, Liu JY, Sze SCW. Comparative analysis of proteins with stimulating activity on ovarian estradiol biosynthesis from four different *Dioscorea* species in vitro using both phenotypic and target-based approaches: Implication for treating menopause. *Appl Biochem Biotechnol* 2016;**180**:79–93.
35. Yoshida R, Nagira M, Kitaura M, Imagawa N, Imai T, Yoshie O. Secondary lymphoid-tissue chemokine is a functional ligand for the CC chemokine receptor CCR7. *J Biol Chem* 1998;**273**:7118–7122.
36. Sarafi MN, Garcia-Zepeda EA, MacLean JA, Charo IF, Luster AD. Murine monocyte chemoattractant protein (MCP)-5: A novel CC chemokine that is a structural and functional homologue of human MCP-1. *J Exp Med* 1997;**185**:99–109.
37. Yuan L, Han J, Meng Q, Xi Q, Zhuang Q, Jiang Y, Yuan L, Han J, Meng Q, Xi Q, Zhuang Q, Jiang Y, Han Y, Zhang B, Fang J, Wu G. Muscle-specific E3 ubiquitin ligases are involved in muscle atrophy of cancer cachexia: An in vitro and in vivo study. *Oncol Rep* 2015;**33**:2261–2268.
38. U.S. Department of Health and Human Services Food and Drug Administration Center for Drug Evaluation and Research (CDER). Guidance for industry estimating the maximum safe starting dose in initial clinical trials for therapeutics in adult healthy volunteers 2005:7.
39. Talbert EE, Cuitiño MC, Ladner KJ, Rajasekera PV, Siebert M, Shakya R, Leone GW, Ostrowski MC, Paleo B, Weisleder N, Reiser PJ, Webb A, Timmers CD, Eiferman DS, Evans DC, Dillhoff ME, Schmidt CR, Guttridge DC. Modeling human cancer-induced cachexia. *Cell Rep* 2019;**28**:1612–1622.e4.
40. von Haehling S, Morley JE, Coats AJS, Anker SD. Ethical guidelines for publishing in the *Journal of Cachexia, Sarcopenia and Muscle*: Update 2021. *J Cachexia Sarcopenia Muscle* 2021;**12**:2259–2261.